Superconducting parameters of $BaPt_{4-x}Au_xGe_{12}$ filled skutterudite

A. Maisuradze,[1,2,*] R. Gumeniuk,[3] W. Schnelle,[3] M. Nicklas,[3]
C. Baines,[1] R. Khasanov,[1] A. Amato,[1] and A. Leithe-Jasper[3]

[1] *Laboratory for Muon Spin Spectroscopy, Paul Scherrer Institut, CH-5232 Villigen PSI, Switzerland*
[2] *Physik-Institut der Universität Zürich, Winterthurerstrasse 190, CH-8057 Zürich, Switzerland*
[3] *Max-Planck-Institut für Chemische Physik fester Stoffe, Nöthnitzer Str. 40, 01187 Dresden, Germany*

We report on a study of the superconducting properties for a series of polycrystalline $BaPt_{4-x}Au_xGe_{12}$ filled skutterudite compounds for $x = 0$, 0.5, 0.75, and 1. Muon spin rotation (μSR) spectroscopy as well as magnetization, specific heat, and electrical resistivity measurements were performed. The magnetic penetration depth λ, the coherence length ξ, and the Ginzburg-Landau parameter κ are evaluated. The temperature dependence of the superfluid density is well described by an s-wave superconducting gap and this classical scenario is supported by the field-independent λ. The gap-to-T_c ratio Δ_0/k_BT_c increases with the Au content from 1.70 for $x = 0$ to 2.1(1) for $x = 1$. By combining μSR, magnetization, and specific heat data, we find that $BaPt_{4-x}Au_xGe_{12}$ compounds are in between the dirty and clean limits with mean free paths of the carriers $l \sim \xi$. Interestingly, resistivity data for $BaPt_4Ge_{12}$ indicate a much higher upper critical field, which is probably due to defects or impurities close to the surface of the crystallites.

PACS numbers: 76.75.+i, 74.70.Dd, 74.25.Ha

I. INTRODUCTION

Filled skutterudite compounds MT_4X_{12} with a framework formed from T (Fe, Ru, Os) and X (P, As, Sb) atoms and "filled" with M atoms (rare-earth, alkaline-earth, or alkali metals) came in focus of recent research activities due to a number of unconventional phenomena.[1–7] In their cubic crystal structure, the filler cations M reside in icosahedral cages formed by tilted TX_6 octahedra. The pronounced vibrational amplitudes of the M atoms have been linked to dynamic scattering mechanisms for heat-carrying acoustic phonons resulting in a reduced lattice thermal conductivity, a prerequisite for thermoelectric applications.[8] Several filled skutterudites display superconductivity and as well show a broad variety of other interesting phenomena.[9–13]

Recently, a new family of filled skutterudites based on a different framework of platinum and germanium with the chemical formula MPt_4Ge_{12} has been discovered.[14,15] Several of these compounds are superconducting (SC). The compositions with M = Sr and Ba[14,15] have SC transition temperatures T_c around 5 K and the later reported $ThPt_4Ge_{12}$ is SC below 4.62 K.[16,17] Due to a peak in the electronic density of states (DOS) at the Fermi energy (E_F), $LaPt_4Ge_{12}$ has a significantly higher T_c of 8.3 K.[15] Interestingly, $PrPt_4Ge_{12}$, with trivalent Pr in a non-magnetic crystal field ground state, is also SC with an only slightly lower T_c of 7.9 K. Its SC properties[18,19] show some similarities with the heavy-fermion superconductivity of $PrOs_4Sb_{12}$.[11,20–22] Most remarkably, an unconventional SC order parameter with point nodes and a rather similar gap-to-T_c ratio has been observed. Moreover, signatures of time-reversal-symmetry breaking were found in $PrPt_4Ge_{12}$ by zero-field μSR.[19]

For $LaPt_4Ge_{12}$, $SrPt_4Ge_{12}$, and $BaPt_4Ge_{12}$, NMR and NQR studies suggested an s-wave BCS SC state with $\Delta_0/k_BT_c \approx 1.60$.[23–25] Theoretical and experimental studies of the electronic structure of this class of skutterudites consistently show rather deep-lying Pt $5d$ states which only partially form covalent bands with Ge $4p$ electrons.[26] In turn, the electronic states at E_F that are relevant for the SC behavior, can be firmly assigned to originate predominantly from Ge $4p$ electrons.[27] Different to MPt_4Ge_{12} (M = La, Pr) a pronounced peak in the DOS is located little above E_F for $SrPt_4Ge_{12}$ and $BaPt_4Ge_{12}$.[28] Here, the low-lying Pt states open up the chance to influence the Fermi level in a rigid-band like manner by a suitable substitution of Pt. By electron doping, the DOS and thus the SC T_c of $BaPt_4Ge_{12}$ could be systematically influenced through substitution of Pt by Au. The T_c in the series $BaPt_{4-x}Au_xGe_{12}$ could be optimized to 7.0 K for $x = 1$.[28] For a doping with more than 1.0 extra electrons per formula unit a decrease of T_c is expected.[28] Actually, the partial substitution of Au for Pt in $LaPt_4Ge_{12}$ leads to a continuous decrease of T_c.[29]

Here, we report on a study of $BaPt_{4-x}Au_xGe_{12}$ compounds ($x = 0$, 0.5, 0.75, and 1) by means of transverse field (TF) muon-spin rotation (μSR) spectroscopy and macroscopic magnetization, specific heat, and electrical resistivity measurements. High-quality μSR spectra of well-ordered SC flux-line lattices allowed us to use the exact solution of the Ginzburg-Landau (GL) equations for the analysis. The superfluid density (ρ_s) was found to saturate exponentially in the low-temperature limit, suggesting a SC gap without nodes, in agreement with a NMR study.[25] The temperature dependence of ρ_s is well described by the s-wave BCS function with the gap-to-T_c ratios (Δ_0/k_BT_c) of 1.70, 2.07, 2.15, and 2.02 for $x = 0$, 0.5, 0.75, and 1, respectively. This clear increase of Δ_0/k_BT_c (viz. electron-phonon coupling) with x is in agreement with the results of our previous study.[28] The BCS character of the superconductivity is further supported by the field-independent magnetic penetration depth (λ). By combining μSR, magnetization and spe-

cific heat data we find that $BaPt_{4-x}Au_xGe_{12}$ compounds are in between the dirty and clean limits with mean free path of the carriers $l \sim \xi$. In electrical resistivity measurements on $BaPt_4Ge_{12}$ we observe superconductivity for fields much higher than the (bulk) upper critical field. This discrepancy appears especially for $x = 0$ samples and its origin is discussed in terms of the presence of chemical or crystallographic defects close to or on the surface of the crystallites.

The paper is organized as follows: in Section II we give some experimental details, Sec. III describes the method of analysis of our μSR data, then we present and discuss the results from the μSR as well as from the macroscopic methods. Our conclusions are given in Sec. IV. In the Appendix we describe the details of our calculations and give the relevant GL definitions.

II. EXPERIMENTAL DETAILS

Polycrystalline samples of $BaPt_{4-x}Au_xGe_{12}$ with bulk T_c values of 4.9(1), 5.3(1), 6.25(5), and 6.95(5) K for $x = 0$, 0.5, 0.75, and 1, respectively, were prepared as described in Refs. 15 and 28. The SC transition temperatures T_c were determined from the onset of the Meissner flux expulsion (field cooling; tangent to the steepest slope and extrapolation to $\chi = 0$) in magnetic susceptibility data measured in a nominal field of 2 mT (MPMS-XL7, Quantum Design).

The transverse field (TF) μSR experiments were performed at the πM3 and μE1 beam lines at the Paul Scherrer Institute (Villigen Switzerland) at the GPS, the LTF, and the GPD spectrometers. Each sample used for the μSR study has an ellipsoid-like shape of a droplet with dimensions: $\simeq 7 \times 7 \times 4$ mm^3, and therefore, field inhomogeneities due to demagnetization are negligible. The samples were field-cooled from above T_c down to 1.6 K in a field of 50 mT and measured as a function of temperature (on the GPS spectrometer). Additional measurements were performed down to $T \simeq 0.29$ K (GPD spectrometer; ^{3}He cryostat) and $T \simeq 0.03$ K (LTF spectrometer; ^{3}He/^{4}He dilution cryostat) in an applied field of 50 mT. Measurements in a series of fields ranging from 10 mT to 640 mT at 1.7 K were also performed. Typical counting statistics were $\approx 6 \times 10^6$ positron events per each data point.

Isothermal magnetization loops at 1.85 K were also recorded on the SQUID magnetometer. In order to reduce demagnetization effects for these measurements splinters of the samples were glued to a quartz capillary with their longest dimensions parallel to the field direction. Specific heat capacity as well as electrical resistance measurements (ac, 93 Hz, current density $j = 0.0072$ A mm^{-2}) at T_c and up to 320 K were performed in magnetic fields up to 2.0 T in a measurement system (PPMS 9, Quantum Design).

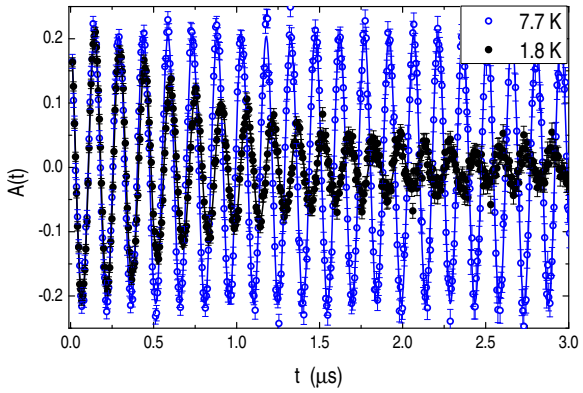

FIG. 1. (Color online) μSR time-spectra below and above $T_c = 6.95$ K in $BaPt_3AuGe_{12}$. The strong relaxation of the signal at 1.8 K is due to the formation of the flux-line lattice. Solid lines are fits to Eq. (2).

III. ANALYSIS, RESULTS, AND DISCUSSION

A. Muon spin rotation data

Figure 1 exhibits typical μSR time spectra measured above and below $T_c = 6.95$ K in $BaPt_3AuGe_{12}$. The spectra of the other samples are similar. Negligibly small muon relaxations above the respective T_c are observed in all samples for the whole field range. A fit with the function $A\cos(\gamma_\mu Bt+\phi)\exp(-1/2\sigma_N^2 t^2)$ results in $\sigma_N \leq 0.06\,\mu$s^{-1} (here, A, B, ϕ, and σ_N are asymmetry, internal field, muon-spin phase, and relaxation rate, respectively). The relaxation rate $\sigma_N < 0.06\,\mu$s^{-1} is mostly due to the nuclear magnetism of Ba, Pt, Au, and Ge isotopes, which causes a weak depolarization of the muon-spin ensemble. Below T_c, all samples exhibit relaxing μSR asymmetry spectra due to the spatial variation of the internal field in the vortex-lattice state induced by the SC condensate. The Fourier transform (FT) of this signal directly shows the field distribution probed by the muon spins.

Figure 2 exhibits the FT spectra in $BaPt_{3.5}Au_{0.5}Ge_{12}$ in a broad range of fields. The asymmetric character of the vortex-lattice field distributions – reflecting the signatures of singularities at the minimum, saddle, and core fields – is clearly visible. Consequently, we analyzed the μSR spectra for all $BaPt_{1-x}Au_xGe_{12}$ samples using the exact solution of the GL equations with the method suggested by Brandt (see Appendix).[30,31] The spatial magnetic field distribution $B(\mathbf{r}) = B(\mathbf{r}, \lambda, \xi, \langle B \rangle)$ within the unit cell of the flux-line lattice (FLL) was obtained by minimization of Eq. (A.1). From the obtained $B(\mathbf{r})$ the probability field distribution for the ideal (defect-free) FLL $P_{\rm id}(B)$ is calculated as follows:

$$P_{\rm id}(B') = \int \delta(B' - B(\mathbf{r}))d\mathbf{r} \qquad (1)$$

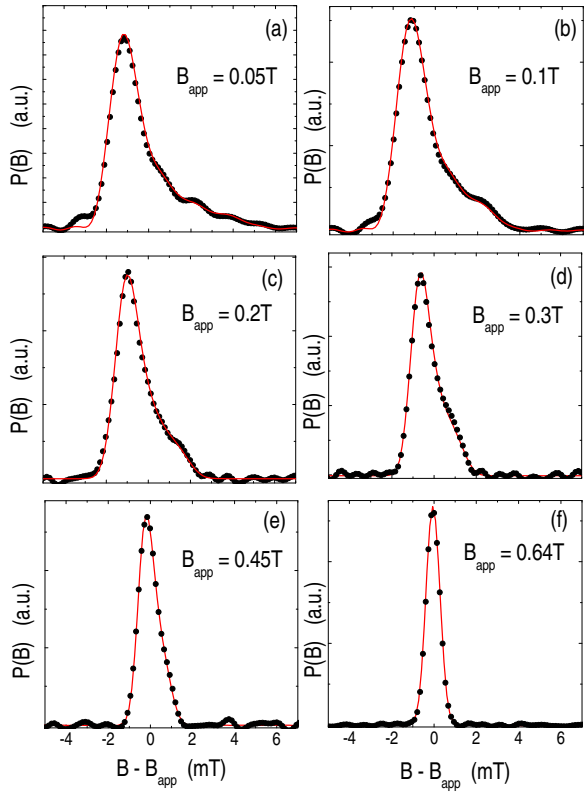

FIG. 2. (Color online) a–f: Fourier transforms (FT) of the μSR time-spectra at 1.7 K in different applied magnetic fields $\langle B\rangle$ = 0.05, 0.1, 0.2, 0.3, 0.45, and 0.64 T for $BaPt_{3.5}Au_{0.5}Ge_{12}$ (corresponding reduced fields are $b = \langle B\rangle/B_{c2}$ = 0.06, 0.12, 0.24, 0.36, 0.54, and 0.76). In this compound, fields close to $B_{c2}(1.7\,\mathrm{K}) = 0.84(4)$ T are reachable. The solid lines are the FT of the fit curves with Eq. (2). The field-dependent spectra are well described by the field-independent parameters $\lambda = 239(4)$ nm and $\xi = 18.8(5)$ nm.

By assuming the internal field distribution $P_{\rm id}(B)$ given by Eq. (1) and accounting for the FLL disorder by multiplying $P_{\rm id}(B)$ to a Gaussian function,[32] one obtains the theoretical polarization function $P(t)$ given by:

$$P(t) = A\exp\left[-\tfrac{1}{2}(\sigma_g^2+\sigma_N^2)t^2\right]\int P_{\rm id}(B)\cos(\gamma_\mu Bt+\phi)dB + A_{\rm bg}\exp\left(-\tfrac{1}{2}\sigma_{\rm bg}^2t^2\right)\cos(\gamma_\mu B_{\rm bg}t+\phi), \quad (2)$$

which was used to fit the μSR time-spectra. Here, $\gamma_\mu = 2\pi\cdot 135.53\,\mathrm{MHz/T}$ is the muon gyromagnetic ratio, A is the asymmetry of the sample signal, ϕ is the phase of the muon-spin ensemble, σ_g is a parameter related to FLL disorder,[33] and σ_N the additional muon depolarization due to the nuclear magnetism of various ions in the samples. The parameters $A_{\rm bg}$, $\sigma_{\rm bg}$, and $B_{\rm bg}$ correspond to asymmetry, relaxation, and field of the background signal, respectively. The asymmetries A and $A_{\rm bg}$ are found to be temperature independent and $A + A_{\rm bg} = 0.20$ (for the GPS and LTF spectrometers) and $A + A_{\rm bg} = 0.27$ (for the GPD spectrometer). The background asymmetry $A_{\rm bg} \simeq 0.004$ is negligibly small for the measurements in the temperature range above 1.7 K (on the GPS spectrometer) while it is substantial in the measurements in the low-temperature range ($A_{\rm bg} \approx 0.07$ on the LTF spectrometer and $A_{\rm bg} \approx 0.20$ on the GPD spectrometer). The magnitude of $\sigma_N \simeq 0.05(1)\,\mu\mathrm{s}^{-1}$ in $BaPt_{1-x}Au_xGe_{12}$ was determined from data above T_c. Zero-field μSR measurements in $BaPt_4Ge_{12}$ and $LaPt_4Ge_{12}$[19] show that the ZF relaxation rate is small and temperature independent, confirming the absence of magnetism. Thus, σ_N is negligibly small in comparison to the muon depolarization caused by the nanoscale field inhomogeneities of the FLL. The background relaxation is also small ($\sigma_{\rm bg} \simeq 0.30$ or $0.007\,\mu\mathrm{s}^{-1}$), since it corresponds to the signals originating from the copper or silver sample-holder and from the walls of the cryostat.

The whole temperature dependence was fitted globally with Eq. (2) with the common parameters A, $A_{\rm bg}$, $B_{\rm bg}$, $\sigma_{\rm bg}$, and σ_N. In addition, the GL parameter $\kappa = \lambda/\xi$ was taken as temperature-independent [*i.e.* the temperature dependent parameters $\xi = \lambda/\kappa$ and $B_{c2} = \Phi_0/2\pi\xi^2$ are related to $\lambda(T)$]. The only temperature-dependent parameters are λ and $\langle B\rangle$. The parameter σ_g can be left free, however, relating $\sigma_g = a/\lambda^2$ with the single global parameter a reduces the total number of parameters, thus reducing the error-bars for λ. Such a relation corresponds to a rigid FLL.[33] For a more detailed description of the fitting procedure we refer to Ref. 34.

The mean value of the superfluid density is related to the magnetic penetration depth as follows (see Appendix): $\rho_s \propto (1-b)/\lambda^2 = 1/\tilde{\lambda}^2$.[18,31] Here, $b = \langle B\rangle/B_{c2}(0)$ is the reduced field and $\tilde{\lambda}$ is the effective magnetic penetration depth.[32] The temperature dependencies of $1/\tilde{\lambda}^2$ for the $BaPt_{4-x}Au_xGe_{12}$ samples are shown in Fig. 3a. The superfluid density saturates exponentially below $\approx T_c/3$. This documents the absence of quasiparticle excitations in the low-temperature limit, which in turn suggests a superconducting gap without nodes in these compounds. In Fig. 3b we show fitting results for $\langle B\rangle$. The magnitude of field inhomogeneity due to demagnetization effects is only a small fraction of $\langle B\rangle - B_{app}$ since shape of each sample is close to an ellipsoid (where internal field is homogeneous).

The low-temperature limit of magnetic penetration depth and upper critical field obtained for $BaPt_4Ge_{12}$ are $\lambda = 204(4)$ nm and $B_{c2} = 0.46(3)$ T (at $T = 1.7$ K), respectively. These values substantially differ from these reported in Ref. 14 $\lambda = 320$ nm and $B_{c2} = 1.8$ T, obtained by magnetization and specific heat measurements, respectively. This discrepancy is explained by substantial scattering of Cooper pairs on nonmagnetic impurities with the mean free path l comparable to the clean-limit coherence length $\xi_{\rm cl}$. Indeed, the coherence length and the magnetic penetration depth are related to these of the clean limit ($l \to \infty$) as follows:[36]

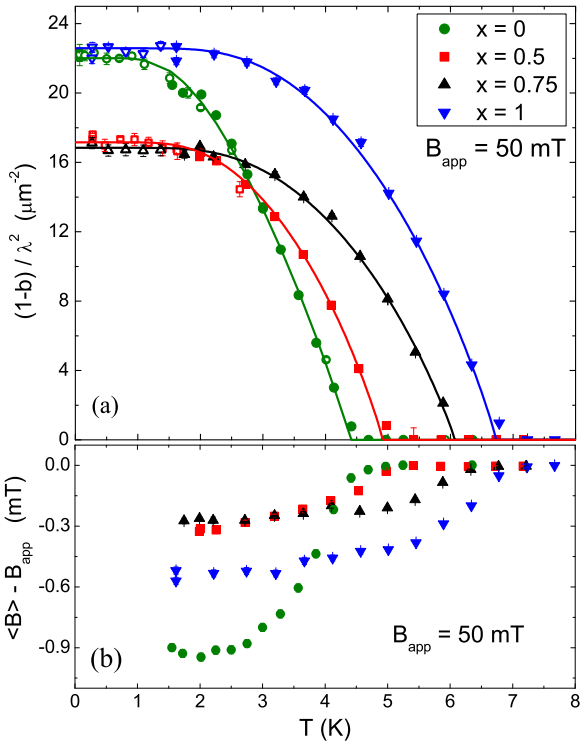

FIG. 3. (Color online) a: Temperature dependence of $(1-b)/\lambda^2 \propto \rho_s$ measured at $B_{\rm app} = 0.05\,$T in $BaPt_{4-x}Au_xGe_{12}$ for $x = 0$, 0.5, 0.75, 1. All compounds exhibit exponential saturation of ρ_s in the low temperature limit, documenting a fully developed gap on the Fermi surface. Solid symbols correspond to measurements above 1.6 K (on the GPS spectrometer) while the empty symbols correspond to those measured in the low temperature limit (on the GPD at $x = 0.5$, 0.75, and 1 and on the LTF at $x = 0$ spectrometers). The solid lines are fits to the Eq. (5). b: Temperature dependence of $\langle B\rangle$ for the samples measured on the GPS spectrometer. Field inhomogeneity due to demagnetization effects are only a small fraction of $\langle B\rangle - B_{\rm app}$.

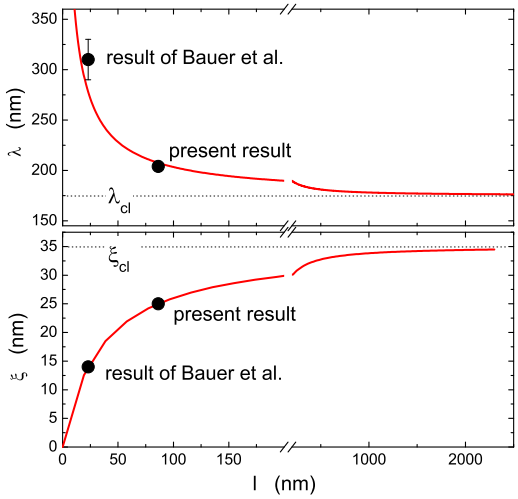

FIG. 4. (Color online) Magnetic penetration depth λ and coherence length ξ of $BaPt_4Ge_{12}$ obtained in present study and by Bauer *et al.*[14] (circles). The solid lines are fits to the data using Eqs. (3)-(4) as described in the text.

$$\xi = \frac{\xi_{\rm cl} l}{\xi_{\rm cl} + l}, \tag{3}$$

$$\lambda = \lambda_{\rm cl}\sqrt{1 + \frac{\xi_{\rm cl}}{l}}. \tag{4}$$

Fitting this equation to the values of ξ_1 and ξ_2 reported in Ref. 14 and obtained here, respectively, with the additional condition $l_1/l_2 = \rho_2^0/\rho_1^0 = 3.75$ (here ρ_i^0 are corresponding residual resistivities) we obtain for $l_1 = 23\,$nm, $l_2 = 86\,$nm and $\xi_{\rm cl} = 35\,$nm (see Fig. 4). Note, here we used the GL relation $B_{c2} = \Phi_0/2\pi\xi^2$ to obtain ξ_i ($i = 1$, 2). These values of mean free paths (l_1 and l_2) explain well also different reports for magnetic penetration depths $\lambda_1 = 320\,$nm and $\lambda_2 = 204\,$nm (see Fig. 4). Consequently, the compound $BaPt_4Ge_{12}$ is in between of clean and dirty-limit superconductors. The residual resistivities of the compounds with $x = 0.5$, 0.75, and 1 are larger than for $x = 0$. Therefore, they are also dirtier than the $BaPt_4Ge_{12}$ compound without Au substitution.

For the analysis of the superfluid density we adopt the BCS s-wave model with arbitrary impurity scattering rate $1/\tau$:[35]

$$\frac{1}{\lambda^2} = \frac{1}{\lambda_0^2}\pi k_B T \sum_{n=-\infty}^{\infty} \frac{1}{Z_n} \frac{\Delta^2(T)}{[\epsilon_n^2 + \Delta^2(T)]^{3/2}}, \tag{5}$$

with

$$Z_n = 1 + \frac{\hbar}{\tau}\frac{1}{\sqrt{\epsilon_n^2 + \Delta^2(T)}}. \tag{6}$$

Here, the classical BCS temperature dependence of the gap was used $\Delta(t) = \Delta_0\delta(t)$ with $\delta(t) = \tanh\{1.82[1.018(t-1)^{0.51}]\}$ (with $t = T/T_c$).[36] k_B and $\hbar$ are Boltzmann and reduced Planck constants, respectively, $\epsilon_n = \pi T(2n+1)$ are Matsubara frequencies while Z_n are renormalization factors for ϵ_n and the superconducting gap Δ. In the extreme cases of the clean ($\tau \to \infty$) and dirty ($\tau \to 0$) limits this equation converges to the classical clean and dirty superconductor curves (see Appendix).[36] For the Fermi velocity[14] $v_F = 52000\,{\rm m\,s^{-1}}$ and mean free path $l = 86\,$nm of $BaPt_4Ge_{12}$ we obtain the scattering time $\tau = 1.6\times10^{-12}\,$s.

The fits of Eq. (5) to $1/\tilde{\lambda}^2$ are shown in Fig. 3a by solid lines. The fit results for Δ_0, T_c, and the low temperature limits of $1/\tilde{\lambda}(0)^2$ are summarized in Table I. As can be seen in the Appendix, there is a correlation between the parameters τ and Δ_0 in Eq. (5). Therefore, for $BaPt_4Ge_{12}$ ($x = 0$) we used $\tau = 1.6\times10^{-12}\,$s as estimate. For the compounds with $x = 0.5$, 0.75, and 1 we used the upper limit of $\tau_{\rm max} = 1.6\times10^{-12}\,$s, since

TABLE I. Summary of fit results with Eq. (5) for T_c and Δ_0 in $BaPt_{4-x}Au_xGe_{12}$, $x = 0$, 0.5, 0.75, 1. In addition, the low-temperature limit of $1/\tilde{\lambda}^2$ and the gap-to-T_c ratio are given.

x	Δ_0 (meV)	T_c (K)	$\tilde{\lambda}^{-2}(0)$ (μm^{-2})	Δ_0/k_BT_c
0	0.65(1)	4.45(3)	22.0(1)	1.70(3)
0.5	0.88(4)	4.93(1)	17.15(7)	2.07(8)
0.75	1.13(5)	6.10(4)	16.84(9)	2.15(6)
1	1.20(5)	6.86(5)	22.6(3)	2.02(9)

they are dirtier than the $BaPt_4Ge_{12}$ compound. The fit of the data was performed for $\tau = \tau_{\max}$ and $\tau \to 0$ (dirty limit, when $\tau \ll \xi_{\rm cl}/v_F$). Thus, we obtain the upper and lower limits of $\Delta_0^{\max}$ and $\Delta_0^{\min}$, respectively. The values of the gap reported in Table I are $\Delta_0 = 0.5(\Delta_0^{\max}+\Delta_0^{\min})$ with errors including the uncertainty in τ and the (much smaller) statistical error.

With increasing Au substitution the T_c increases, however the gap-to-T_c ratio Δ_0/k_BT_c increases more suddenly and remains essentially unchanged for the Au substitutions $x = 0.5$, 0.75, and 1. The T_c of phonon-mediated SC may be described within the McMillan formula.[36] The Debye temperature is practically the same for our four compounds.[28] Thus, the only factor determining the increase of T_c is the electronic DOS at the Fermi level, which significantly increases with Au substitution beyond $x = 0.4$ (cf. Fig. 1 in Ref. 28).

Another interesting feature is the dependence of the superfluid density upon Au substitution. With increasing x, $\rho_s(0)$ first decreases, goes through a minimum, and then increases with further increasing x. Such a behavior is rather unusual and contrasts with previous observations of a power-law-like relation between T_c and the superfluid density in cuprate high-T_c superconductors,[37] NbB_2,[38] MgB_2,[39] or predicted theoretically.[40,41] However, in the present case such a behavior can be understood. The superfluid density and the magnetic penetration depth λ are dependent on the scattering rate of the Cooper pairs τ (or the mean free path l) [see Eq. 3]. Therefore, the minimum in $\rho_s(0)$ is probably due to the dependence of τ on the Au content x.

Further information about the order parameter can be obtained from the field dependence of the superfluid density. As it is known for superconductors with nodes in the gap, a significant field dependence of λ is observed,[43] while for the large number of classical BCS superconductors λ is field-independent.[44] A fit of the μSR-time spectra at different fields and for $T = 1.7$ K using Eq. (2) results in field-independent values of λ.[45] For the fit the field-independent value of ξ obtained from the GL relation $B_{c2} = \Phi_0/2\pi\xi^2$ was used. Therefore, we next fitted the whole field dependence of the spectra globally with common parameters λ and ξ. Note that the values of the GL parameter $\kappa = \lambda/\xi$ used in the fit of the temperature dependence were obtained from the fit of the corresponding field scan. In Fig. 2 we show the FT μSR spectra for the $BaPt_3AuGe_{12}$ compound at $T = 1.7$ K for the broad range of reduced fields $b = B/B_{c2} = 0.06$, 0.12, 0.24, 0.36, 0.54, and 0.76. The fit results in field-independent values of the magnetic penetration depth ($\lambda = 239(4)$ nm) and of the coherence length ($\xi = 18.8(5)$ nm). This value of ξ is in good agreement with that obtained by the GL relation from the corresponding B_{c2} ($B_{c2} = \Phi_0/2\pi\xi^2$). The fit results for λ, ξ, and κ in $BaPt_{4-x}Au_xGe_{12}$ for $x = 0$, 0.5, 0.75, and 1 are summarized in Table II. The upper critical field for $x = 1$ is in fair agreement with the value given in our previous work,[28] but for $BaPt_4Ge_{12}$ the $B_{c2}(0)$ is much lower than previously reported.[14,28] This drastic discrepancy is investigated and discussed in the following section.

TABLE II. Magnetic penetration depth (λ) and coherence length (ξ) obtained from the global fit of the data in the field range of 0.05 to 0.64 T at 1.7 K. In addition, the values for B_{c2} at $T = 1.7$ K, Ginzburg-Landau parameter $\kappa = \lambda/\xi$, and residual resistivity ρ_0 are listed.

x	λ (nm)	ξ (nm)	κ	$B_{c2}(1.7\,\text{K})$ (T)	ρ_0 ($\mu\Omega$ cm)
0	204(4)	25.5(15)	8.0(5)	0.46(3)	15.1
0.5	239(4)	18.8(9)	12.7(7)	0.84(4)	33.6
0.75	240(4)	15.0(9)	16.0(9)	1.68(5)	36.8
1	210(4)	13.4(8)	15.7(9)	1.93(5)	31.5

B. Macroscopic measurement data

Previously, for $BaPt_4Ge_{12}$ an upper critical field $B_{c2}(0)$ of about 2.0 T was reported by our group, mainly based on $T_c(B_{\rm app})$ data from resistivity measurements in fixed applied fields $B_{\rm app}$.[28] This value was confirmed by similar data of Bauer *et al.*[14] [$B_{c2}(0) = 1.8$ T] from both resistivity *and* specific heat data in field.[14] However, the T_c reported for $BaPt_4Ge_{12}$ in Ref. 14 is 5.35 K (from both resistivity *and* specific heat), which is inconsistent with the magnetic onset $T_c \approx 4.9$ K of our present and $T_c \approx 5.0$ K of our previous $x = 0$ samples. The origin of the drastically different upper critical field values as well as of the unusually large variation of T_c for $BaPt_4Ge_{12}$ samples remained unclear. For this reason we (re-)investigated the present $BaPt_4Ge_{12}$ ($x = 0$) sample as well as the $x = 0$ and $x = 1$ samples from our previous study[28] by macroscopic probes (magnetization, specific heat, electrical resistivity).

An isothermal magnetization loop at $T = 1.85$ K for the $BaPt_4Ge_{12}$ sample used for the μSR measurements is given in Fig. 5. It shows the typical picture of a type II superconductivity with medium large GL parameter κ. A weak second peak effect in $M(B_{\rm app})$ is observed

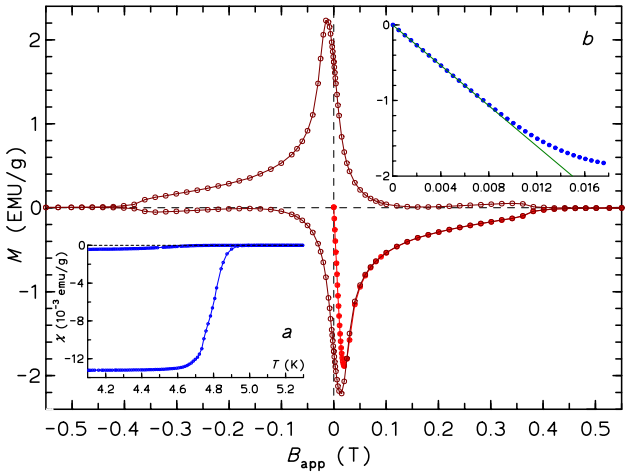

FIG. 5. (Color online) Magnetization loop of $BaPt_4Ge_{12}$ at $T = 1.85\,\mathrm{K}$ up to $B_{\mathrm{max}} = \pm 2.0\,\mathrm{T}$. The initial curve is marked by (light-red) full circles, the other segments by (dark-red) open circles. Inset a: Zero-field cooled (Meissner effect) and field-cooled (shielding) susceptibility in a nominal field of 2 mT. Inset b: low-field magnetization showing the deviation from the initial linear behavior (straight line) at B_{c1}.

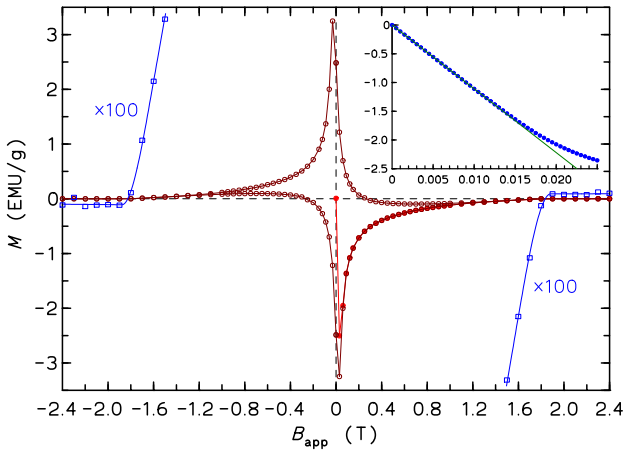

FIG. 6. (Color online) Magnetization loop of $BaPt_3AuGe_{12}$ at $T = 1.85\,\mathrm{K}$ up to $B_{\mathrm{max}} = \pm 3.0\,\mathrm{T}$. The (blue) squares (with a line as guide to the eye) show a 100-fold magnification of the data close to B_{c2}. Inset: low-field magnetization showing the deviation from the initial linear behavior (straight line) used for estimating B_{c1}.

around 0.35 T, indicating relatively weak flux-line pinning in a pure sample.[46] Above this field the hysteresis drastically diminishes (this field is often taken as upper critical field B_{c2})[46] and becomes reversible above $B_{\mathrm{app}} = 500(30)\,\mathrm{mT}$. The reversible SC magnetization decreases to a value of less than 1/1000 of the maximum magnetization signal (the noise level of the measurement) at $B_{\mathrm{app}} = 540(50)\,\mathrm{mT}$, which we adopt as the upper critical field $B_{c2}(1.85\,\mathrm{K})$. Considering the only slightly different temperatures, this value is compatible with $B_{c2}(0)$ from our μSR investigation (see Table II).

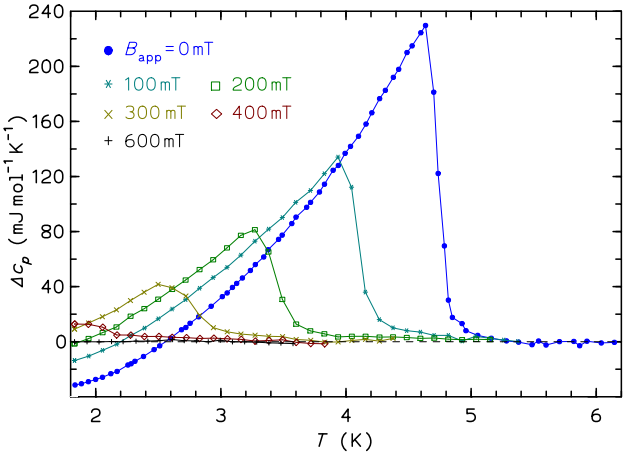

FIG. 7. (Color online) Difference of the specific heat $\Delta c_p(T, B_{\mathrm{app}})$ of $BaPt_4Ge_{12}$ (sample from μSR investigation) between SC and normal state ($B_{\mathrm{app}} = 2.0\,\mathrm{T}$). $\Delta c_p = 0$ is indicated by a dashed line.

The lower critical field can be estimated from the first deviation of $M(B_{\mathrm{app}})$ from linearity (Fig. 5b). Adopting a 0.5 % criterion for a significant deviation, we find $B_{c1} = 6.0(1.0)\,\mathrm{mT}$, again for $T = 1.85\,\mathrm{K}$. This experimental value for B_{c1} is, however, only a lower limit due to the strong influence of the demagnetization effect for a nearly perfect diamagnet. From the B_{c2} value determined from magnetization and $\kappa = 8.0$ from Table II we obtain with the relation $B_{c2} = \sqrt{2}\kappa B_{\mathrm{c,th}}$ a thermodynamic critical field $B_{\mathrm{c,th}} \approx 48\,\mathrm{mT}$, which is clearly larger than the value calculated from the free enthalpy difference from specific heat ($\approx 40\,\mathrm{mT}$ for $T = 1.85\,\mathrm{K}$). Using $B_{c1} \approx (\ln\kappa + 0.5)B_{\mathrm{c,th}}/2\kappa$ (valid for small κ)[30] we find $B_{c1} = 7.7\,\mathrm{mT}$, in fair agreement with the estimate from the magnetization curve. Only slightly different values for the critical fields were obtained from similar magnetization data (not shown) taken on the $BaPt_4Ge_{12}$ sample used in Ref. 28 ($B_{c1} = 4.2(1.0)\,\mathrm{mT}$, $B_{c2} = 590(50)\,\mathrm{mT}$, both at $T = 1.85\,\mathrm{K}$).

The magnetization curve for the $BaPt_3AuGe_{12}$ sample ($x = 1$) of the present study is given in Fig. 6. There is no visible second peak effect and, thus, the upper critical field can be determined accurately from the sharp kinks in $M(B_{\mathrm{app}})$ ($B_{c2} = 1820(20)\,\mathrm{mT}$; see 100-fold magnification of the data in Fig. 6). The estimated B_{c1} is $11.5(1.0)\,\mathrm{mT}$ ($T = 1.85\,\mathrm{K}$; criterion 0.5 % deviation). While the B_{c2} value is only slightly lower compared to the one in Table II the GL parameter $\kappa \approx 13.1$ is clearly lower than the value determined by μSR spectroscopy. The $B_{\mathrm{c,th}}$ calculated using κ from Table II and B_{c2} from the magnetization curve is $\approx 99\,\mathrm{mT}$, which is again clearly larger than the value derived from the specific heat data ($\approx 79\,\mathrm{mT}$ at 1.85 K).

In Fig. 7 the difference specific heat $\Delta c_p(T) = c_p(B_{\mathrm{app}}) - c_p(B > B_{c2})$ is plotted for the present $BaPt_4Ge_{12}$ sample. For fields $\geq 600\,\mathrm{mT}$ no SC signal is observed above our lowest temperature of 1.8 K. The

midpoints of the second-order-type transitions $T_c(B_{\rm app})$ were evaluated. The quadratic extrapolation of these data for $B_{c2}(T)$ to zero temperature results in $B_{c2}(0) = 470(50)\,$mT, in excellent agreement with the values from μSR and magnetization. For the sample used in Ref. 28 we extrapolate $B_{c2}(0) = 540(50)\,$mT. Specific heat data in field for the other compositions are given in Ref. 28.

The electrical resistivity of the present $x = 0$ sample at 300 K is $\approx 90\,\mu\Omega$m with a residual resistance ratio 6.1 (Fig. 8b). Such low RRR values are not typical for polycrystalline samples of other MPt$_4$Ge$_{12}$ compounds (cf. RRR = 33 or 42 [15], RRR $\approx$ 100 [16], or RRR $\geq$ 100 [47]). Obviously, the crystalline quality of polycrystalline BaPt$_4$Ge$_{12}$ samples is worse compared to that of other members of the family of filled Pt-Ge skutterudites. RRR $\approx$ 6 however indicates that a BaPt$_4$Ge$_{12}$ sample with a clearly lower defect concentration than in Refs. 14 or 48 has been achieved. For the present sample the SC transition in $\rho(T, B_{\rm app})$ decreases continuous with increasing field, except for very low fields (Fig. 8a). The onset, mid, and zero-resistance temperatures are plotted against $B_{\rm app}$ in Fig. 8c. Surprisingly, the transition in $\rho(T)$ is still complete for a field of 1.0 T and the onset is even visible at 1.9 K in 1.8 T. Such high upper critical fields are in agreement with the conclusions in Refs. 14, but in strong contrast to the consistently much lower B_{c2} values obtained from the bulk-probes μSR, magnetization, and specific heat. A quadratic extrapolation of $T_{\rm c,mid}$ (range of fit 0.2–1.2 T) to zero temperature results in $B_{c2}^{\rm res}(0) = 1460\,$mT (dashed line in Fig. 8c). In addition, a clear anomaly is seen for the lowest fields, where the resistive T_c is almost 0.5 K higher than expected from the extrapolation curve. Actually, the extrapolated resistive $T_{\rm c,mid}(0) \approx 4.74\,$K agrees well with that from the bulk measurements. For the sample of BaPt$_3$AuGe$_{12}$ no significant discrepancy between bulk and resistive value for B_{c2} are found (see Ref. 28)

What is the origin of this discrepancy in the B_{c2} and $T_c(0)$ values from bulk properties and resistivity in BaPt$_4$Ge$_{12}$? In the low-field susceptibility ($B_{\rm app} = 2\,$mT, μSR sample) a bulk T_c onset of 4.87 K is observed (determined by the tangent to the steepest slope of the field-cooling Meissner transition). However, above $\approx$ 5.0 K there is still a very weak diamagnetic signal, which vanishes exponentially with increasing temperature. The signal is only little weaker in field-cooling than measured after zero-field cooling (zfc), but the maximum of this zfc signal is about 3 orders of magnitude lower than the zfc signal at 4.0 K (or 1.5 orders of magnitude weaker than the bulk Meissner effect).

This weak diamagnetism, the concomitant zero electrical resistance, and the too large B_{c2} value from resistivity data may root in two phenomena: i. the presence of a minor SC impurity phase which forms a percolating SC network with an about 0.5 K higher $T_c(0)$ and much higher B_{c2} than the main phase, or, ii., strong classical surface superconductivity of the main phase with a critical field $B_{c3}(0) \gg B_{c2}(0)$. The second possibility seems to be unlikely due to the facts that $T_{\rm c,bulk}(0) \neq T_{\rm c,surface}$ and that the required surface critical field B_{c3} would well need to exceed the Saint-James–de Gennes limit of $\approx 1.7 B_{c2}$.[49]

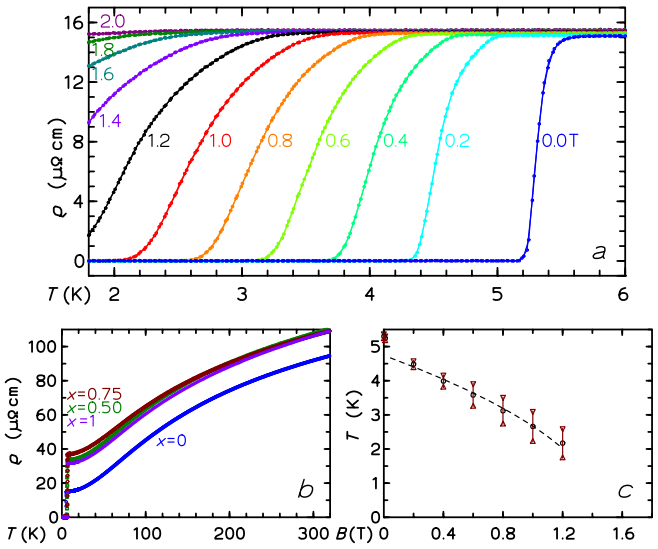

FIG. 8. (Color online) a: Electrical resistivity $\rho(T, B_{\rm app})$ around T_c of the present BaPt$_4$Ge$_{12}$ sample for different applied fields. b: Electrical resistivity $\rho(T)$ in zero field for the $x = 0$, 0.50, 0.75, and 1 samples. c: Variation of the onset, mid (circles), and zero-resistance temperatures with applied field. The dashed line is a quadratic fit for $T_{\rm c,mid}(B_{\rm app})$.

For BaPt$_4$Ge$_{12}$ no homogeneity range is observed since the lattice parameter of the filled-skutterudite phase in a sample with composition Ba$_{0.9}$Pt$_4$Ge$_{12}$ is 8.6837(3) Å, which is practically the same as for BaPt$_4$Ge$_{12}$.[26] Extended EDXS analyses on metallographic polished surfaces of the present BaPt$_4$Ge$_{12}$ sample result in a composition Ba$_{0.9(1)}$Pt$_{4.0(1)}$Ge$_{11.9(1)}$, which agrees very well with the nominal one. Interestingly, there is a significant difference of the lattice parameter of all our BaPt$_4$Ge$_{12}$ samples (present sample $a = 8.6838(5)\,$Å) with that reported by Bauer *et al.*[14] ($a = 8.6928(3)\,$Å),[14] which we currently cannot explain.

The currently studied large BaPt$_4$Ge$_{12}$ sample contains besides the BaPt$_4$Ge$_{12}$ main phase also some BaPtGe$_3$ (no superconductivity observed above 1.8 K),[50,51]. The content of this phase is estimated from Rietveld refinements to be about 4 %. Five weak lines in the X-ray diffraction pattern belong to PtGe$_2$. These lines are too weak to refine a phase content, therefore we estimate a PtGe$_2$ phase fraction of below 2 %. PtGe$_2$ is reported to be a superconductor with $T_c = 0.4\,$K.[52] The presence of these minority phases in the BaPt$_4$Ge$_{12}$ sample thus also cannot explain the observation of a higher upper critical field value in resistivity data.

The resistive percolation (a SC path) at a higher temperature than the bulk T_c hints at a modification of the surface layers of the grains of the majority skutterudite phase, probably due to crystallographic defects or strain. These effects will result in a larger scattering rate and a

shorter mean free path of the charge carriers, thus making the superconductor dirtier, subsequently enlarging the effective penetration depth well above the bulk value.

Since the present samples are polycrystalline pieces, an estimate of the mean free path from the residual resistivity values by the standard formula[53] is problematic and gives at best a lower limit for l. Moreover, skutterudites are not simple metals which can be treated in a one-band model. Our estimate of the minimal mean free path in $BaPt_{4-x}Au_xGe_{12}$ using a free-electron model results in $l_{\rm min} \approx 25$, 14, 14, and 19 nm for $x = 0$, 0.5, 0.75, and 1, respectively.[54] In view of these values of $l_{\rm min}$, the superconductivity in the bulk of the crystallites is neither in the clean nor in the dirty limit. On the surface, however, the superconductivity seems to be in the dirty limit, leading to much shorter coherence lengths than in the bulk. Hence, crystalline defects or impurities on the grain surfaces probably lead to the higher upper critical field value in resistivity data. An open question is the clearly higher T_c of these grain surfaces. The T_c of a superconductor with defects is – in most cases – lower than the T_c of the pure material, however, it is also known that strain, especially on surfaces, can drastically enhance the T_c. While the growth of single crystals of sufficient size of $BaPt_4Ge_{12}$ was not successful until now, investigations on such crystals would be highly desirable.

IV. CONCLUSION

We performed an investigation using transverse-field μSR spectroscopy for a series of polycrystalline $BaPt_{4-x}Au_xGe_{12}$ superconductors with $x = 0$, 0.5, 0.75, and 1. Highly asymmetric μSR time spectra were analyzed within the framework of the Ginzburg-Landau (GL) theory by precise minimization of the GL free energy.[31] Zero-temperature magnetic penetration depths [$\lambda(0)$] and GL parameters ($\kappa = \lambda/\xi$) were evaluated (see Table II). The temperature dependence of the superfluid density ρ_s in all the compounds saturates exponentially in the low-temperature limit, which documents the absence of nodes in the superconducting gap function. This finding is in agreement with the results of a previous NMR study.[25] Our analysis shows that ρ_s is well described within the classical s-wave BCS model with gap-to-T_c ratios (Δ_0/k_BT_c) of 1.70, 2.07, 2.15, and 2.02 for $x = 0$, 0.5, 0.75, and 1, respectively. These ratios are in fair agreement with the reduced specific heat jump $\delta c_p/\gamma_N T_c$ from our previous study.[28] The observation of field-independent λ values further supports the classical s-wave pairing scenario for these compounds. Thus, the present experimental results from bulk probes point to the classical s-wave phonon-mediated superconductivity for all compounds in the series $BaPt_{4-x}Au_xGe_{12}$ up to $x = 1$. The upper critical field data from the μSR study are in good agreement with bulk-sensitive thermodynamic measurements of the upper critical fields of $BaPt_4Ge_{12}$ and $BaPt_3AuGe_{12}$. The origin of much higher upper critical fields observed in electrical resistivity measurements for the present $BaPt_4Ge_{12}$ sample (as in previous reports[14,15,28]) is due to a larger carrier scattering rate at the surface of the crystallites.

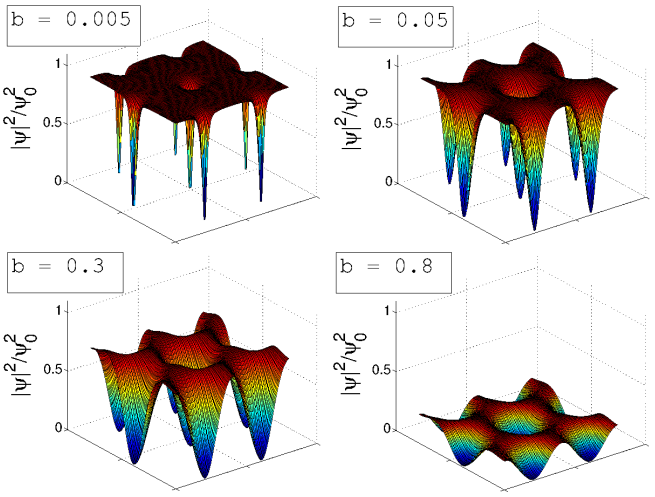

FIG. 9. (Color online) Spatial variation of the normalized superfluid density $|\psi(\mathbf{r})|^2/\psi_0^2$ in a hexagonal FLL at four different reduced fields $b = \langle B\rangle/B_{c2}$. The minima of $|\psi(\mathbf{r})|^2$ correspond to positions of vortex cores.

ACKNOWLEDGEMENTS

We would like to acknowledge fruitful discussions concerning GL theory with the late E. H. Brandt. This work was partly performed at the Swiss Muon Source (SμS), Paul Scherrer Institut (PSI, Switzerland). The work was supported by the NCCR program *Materials with Novel Electronic Properties* (MaNEP) sponsored by the Swiss National Science Foundation. We acknowledge helpful discussions with H. Rosner and thank Yu. Grin for continuous support of our work.

Appendix: Details of calculations and GL definitions

Below we describe some details of our calculations and introduce the basic definitions of the Ginzburg-Landau (GL) theory used in this analysis. As shown by Abrikosov, a type II superconductor forms a periodic vortex or flux-line lattice (FLL) in a range of magnetic fields (B).[55] Here, $B_{c1} < B < B_{c2}$, where B_{c1} and B_{c2} are the lower and upper critical fields, respectively. The GL theory used by Abrikosov occurred to be one of the most useful approaches for the evaluation of the field distribution in a type II superconductor (although it is strictly valid only close to T_c) and forms the basis for the analysis of transverse field (TF) μSR data.

For the limiting cases of $\kappa \to \infty$ ($\kappa = \lambda/\xi$ is the GL parameter) and $B_{c1} < B \ll B_{c2}$ simplified, sec-

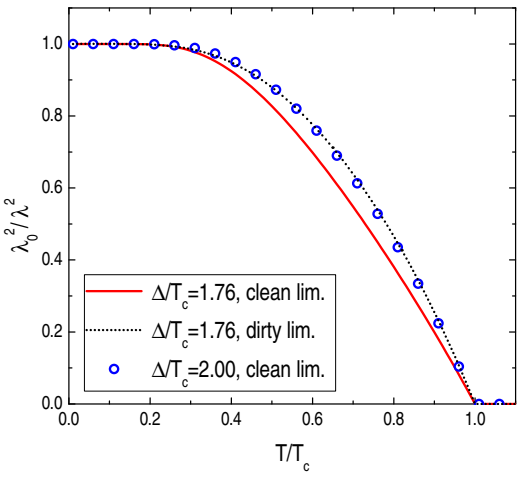

FIG. 10. (Color online) Temperature dependence of normalized superfluid density $\lambda_0^2/\lambda^2(t)$ in clean and dirty limits ($t = T/T_c$). In open circles $\lambda_0^2/\lambda^2(t)$ in the clean limit but larger gap-to-T_c ratio is shown.

ond moment analysis methods were developed.[30,56] In the general case of arbitrary κ and B, the solution is more complicated and various approximations have been suggested.[32,57–61] A feasible and precise minimization algorithm of the "classical" GL free energy has been suggested by Brandt.[31] The method was first used in the experimental work in Ref. 62. The difference between the SC and the normal-state free energies $\Delta F = F_s - F_n$ is expressed as (in SI units):[31,36,63]

$$\Delta F = \alpha|\psi|^2 + \frac{\beta}{2}|\psi|^4 + \frac{1}{2m^*}\left|\left(\frac{\hbar}{i}\nabla - 2e\mathbf{A}\right)\psi\right|^2 + \frac{\mathbf{B}^2}{2\mu_0}. \quad \text{(A.1)}$$

Here, $\mathbf{B} = \mathrm{rot}\mathbf{A}$, the parameter $\beta = \mu_0/2\cdot(\kappa e\hbar/m)^2$ is determined by the GL parameter κ, and $\psi_0^2 = -\alpha/\beta > 0$. The parameter ψ_0^2 is the superfluid density deep in the bulk of the superconductor in the limit of low fields (i.e. in the Meissner state), which is related to the magnetic penetration depth λ. The relation between λ^{-2} and ψ_0^2 is (in SI units):[63]

$$\lambda^{-2} = \frac{4\mu_0 e^2}{m^*}\psi_0^2. \quad \text{(A.2)}$$

In an applied field, however, the superfluid density $|\psi|^2$ is spatially inhomogeneous with minima at the vortex cores due to the formation of a FLL.[55] Fig. 9 shows the spatial variation of $|\psi(\mathbf{r})|^2/\psi_0^2$ at different reduced fields $b = \langle B\rangle/B_{c2}$ in the limit of $\kappa \to \infty$ corresponding to the minimum of Eq. (A.1) ($\langle B\rangle$ is the mean field in the sample). Although λ is field-independent (as well as α and β) and finite at $T = T_c^{B_{c2}} \equiv T_c(B \neq 0)$, the superfluid density reduces with increasing field and vanishes at $T = T_c^{B_{c2}}$. Therefore, with increasing field for $b \gtrsim 0.05$ (e.g. for a non-high-T_c superconductor; see Fig. 9) the correction factor $(1-b)$ to the superfluid density becomes significant. The mean value of the superfluid density reduces with increasing field as follows:[30,31]

$$\rho_s = \langle|\psi|^2\rangle \simeq (1-b)\psi_0^2. \quad \text{(A.3)}$$

For small values of $b \to 0$ and high κ, as in most of the high-T_c superconductors, we have $\rho_s \propto \lambda^{-2}$. In the present analysis the free energy [Eq. (A.1)] for the given λ, ξ, and $\langle B\rangle$ was minimized using the method suggested by Brandt.[31] This results in a solution for spatial variation of the field $\mathbf{B}(\mathbf{r})$ and the order parameter $\psi(\mathbf{r})$.

Appendix: Some details on Eq. (5)

We use Eq. (5) suggested in Ref. 35 for the case of arbitrary scattering rate $1/\tau$ (mean free path $l = v_F\tau$). For the classical BCS gap-to-T_c ratio $\Delta_0/k_BT_c = 1.76$ the temperature dependence of the normalized superfluid density $\lambda_0^2/\lambda^2(t)$ obtained with Eq. (5) in clean ($\tau \gg \xi_{\rm cl}/v_F$) and dirty ($\tau \ll \xi_{\rm cl}/v_F$) limit is given in Fig. 10 ($t = T/T_c$). The results are in good agreement with curves given in Ref. 36. Note, the shape of $\lambda_0^2/\lambda^2(t)$ depends on the scattering rate only for $\tau \sim \xi_{\rm cl}/v_F$. For the current precision of measurement the parameters Δ_0 and τ are correlated. The dirty-limit curve with $\Delta_0/k_BT_c = 1.76$ can be well fitted with the clean-limit model with $\Delta_0/k_BT_c = 2.0$ (see Fig. 10).

* alexander.maisuradze@psi.ch

[1] B. C. Sales: in *Handbook on the Physics and Chemistry of Rare Earths*, eds. K. A. Gschneider, Jr., J.-C. G. Bunzli, and V. K. Pecharsky, Vol. 33, p. 1–34 (Elsevier, Amsterdam, 2003).

[2] Y. Aoki, H. Sugawara, H. Harima, and H. Sato, J. Phys. Soc. Jpn. **74**, 209 (2005).

[3] M. B. Maple, J. Phys. Soc. Jpn. **74**, 222 (2005).

[4] H. Sato, D. Kikuchi, K. Tanaka, H. Aoki, K. Kuwahara, Y. Aoki, M. Kohgi, H. Sugawara, and K. Iwasa, J. Magn. Magn. Mater. **310**, 188 (2007).

[5] C. Uher, Semicond. Semimet. **69**, 139 (2001).

[6] W. Jeitschko, D. Braun, Acta Cryst. **B33**, 3401 (1977).

[7] A. Leithe-Jasper, W. Schnelle, H. Rosner, M. Baenitz, A. Rabis, A. A. Gippius, E. N. Morozova, H. Borrmann, U. Burkhardt, R. Ramlau, U. Schwarz, J. A. Mydosh, Yu. Grin, V. Ksenofontov, and S. Reiman, Phys. Rev. B **70**,

214418 (2004).
[8] G. S, Nolas, D. T. Morelli, T. M. Tritt, Ann. Rev. Mater. Sci. **29**, 89 (1999).
[9] G. P. Meisner, Physica B+C (Amsterdam) **108**, 763 (1981). L. E. Delong and G. P. Meisner, Solid State Commun. **53**, 119 (1985).
[10] T. Uchiumi, I. Shirotani, Ch. Sekine, S. Todo, T. Yagi, Y. Nakazawa, and K. Kanoda, J. Phys. Chem. Solids **60**, 689 (1999).
[11] E. D. Bauer, N. A. Frederick, P.-C. Ho, V. S. Zapf, and M. B. Maple, Phys. Rev. B **65**, 100506(R) (2002).
[12] I. Shirotani, Y. Shimaya, K. Kihou, C. Sekine, N. Takeda, M. Ishikawa, and T. Yagi, J. Phys.: Condens. Matter **15**, s2201 (2003).
[13] I. Shirotani, S. Sato, C. Sekine, K. Takeda, I. Inagawa, and T. Yagi, J. Phys.: Condens. Matter **17**, 7353 (2005).
[14] E. Bauer, A. Grytsiv, X.-Q. Chen, N. Melnychenko-Koblyuk, G. Hilscher, H. Kaldarar, H. Michor, E. Royanian, G. Giester, M. Rotter, R. Podloucky, and P. Rogl, Phys. Rev. Lett. **99**, 217001 (2007).
[15] R. Gumeniuk, W. Schnelle, H. Rosner, M. Nicklas, A. Leithe-Jasper, and Yu. Grin, Phys. Rev. Lett. **100**, 017002 (2008).
[16] D. Kaczorowski and V. H. Tran, Phys. Rev. B **77**, 180504(R) (2008).
[17] E. Bauer, X.-Q. Chen, P. Rogl, G. Hilscher, H. Michor, E. Royanian, R. Podloucky, G. Giester, O. Sologub, and A. P. Gonçalves, Phys. Rev. B **78**, 064516 (2008).
[18] A. Maisuradze, M. Nicklas, R. Gumeniuk, C. Baines, W. Schnelle, H. Rosner, A. Leithe-Jasper, Yu. Grin, and R. Khasanov, Phys. Rev. Lett. **103**, 147002 (2009).
[19] A. Maisuradze, W. Schnelle, R. Khasanov, R. Gumeniuk, M. Nicklas, H. Rosner, A. Leithe-Jasper, Yu. Grin, A. Amato, and P. Thalmeier, Phys. Rev. B **82**, 024524 (2010).
[20] Y. Aoki, A. Tsuchiya, T. Kanayama, S. R. Saha, H. Sugawara, H. Sato, W. Higemoto, A. Koda, K. Ohishi, K. Nishiyama, and R. Kadono, Phys. Rev. Lett. **91**, 067003 (2003).
[21] M. B. Maple, Z. Henkie, W. M. Yuhasz, P.-C. Ho, T. Yanagisawa, T. A. Sayles, N. P. Butch, J. R. Jeffries, and A. Pietraszko, J. Magn. Magn. Mater. **310**, 182 (2007). M. B. Maple, N. A. Frederick, P.-C. Ho, W. M. Yuhasz, and T. Yanagisawa, J. Supercond. Novel Magn. **19**, 299 (2006).
[22] H. Sugawara, S. Osaki, S. R. Saha, Y. Aoki, H. Sato, Y. Inada, H. Shishido, R. Settai, Y. Onuki, H. Harima, and K. Oikawa, Phys. Rev. B **66**, 220504(R) (2002).
[23] F. Kanetake, H. Mukuda, Y. Kitaoka, H. Sugawara, K. Magishi, K. M. Itoh, and E. E. Haller, Physica C **470**, 703 (2009); *idem ibid* J. Phys. Soc. Jpn. **79**, 063702 (2010).
[24] M. Toda, H. Sugawara, K. Magishi, T. Sato, K. Koyama, Y. Aoki, and H. Sato, J. Phys. Soc. Japan **77**, 124702 (2008).
[25] K. Magishi, H. Sugawara, N. Ohta, T. Saito, K. Koyama, Physica C **470**, 552 (2009).
[26] R. Gumeniuk. H. Borrmann, A. Ormeci, H. Rosner, W. Schnelle, M. Nicklas, Yu. Grin, A. Leithe-Jasper, Z. Kristallogr. **225**, 531-543 (2010).
[27] H. Rosner, J. Gegner, D. Regesch, W. Schnelle, R. Gumeniuk, A. Leithe-Jasper, H. Fujiwara, T. Haupricht, T. C. Koethe, H.-H. Hsieh, H.-J. Lin, C. T. Chen, A. Ormeci, Yu. Grin, and L. H. Tjeng, Phys. Rev. B **80**, 075114 (2009).
[28] R. Gumeniuk, H. Rosner, W. Schnelle, M. Nicklas, A. Leithe-Jasper, and Yu. Grin, Phys. Rev. B **78**, 052504 (2008).
[29] L. Li, E. Sakada, and K. Nishimura, Mater. Trans. **51**, 227 (2010).
[30] E. H. Brandt, Phys. Rev. B **68**, 054506 (2003).
[31] E. H. Brandt, Phys. Rev. Lett. **78**, 2208 (1997).
[32] E. H. Brandt, J. Low Temp. Phys. **26**, 709 (1977); *idem ibid* **73**, 355 (1988).
[33] T. M. Riseman, J. H. Brewer, K. H. Chow, W. N. Hardy, R. F. Kiefl, S. R. Kreitzman, R. Liang, W. A. MacFarlane, P. Mendels, G. D. Morris, J. Rammer, J. W. Schneider, C. Niedermayer, and S. L. Lee, Phys. Rev. B **52**, 10569 (1995).
[34] A. Maisuradze, R. Khasanov, A. Shengelaya, and H. Keller, J. Phys.: Condens. Matter **21**, 075701 (2009).
[35] D. Xu, S.K. Yip, and J.A. Sauls, Phys. Rev. B **51**, 16233 (1995).
[36] M. Tinkham, *Introduction to Superconductivity*, Krieger Publishing, Malabar FL (1975).
[37] Y. J. Uemura *et al.* Phys. Rev. Lett. **62**, 2317 (1989).
[38] R. Khasanov, A. Shengelaya, A. Maisuradze, D. Di Castro, R. Escamilla, and H. Keller, Phys. Rev. B **77**, 064506 (2008).
[39] S. Serventi, G. Allodi, R. De Renzi, G. Guidi, L. Romanò, P. Manfrinetti, A. Palenzona, Ch. Niedermayer, A. Amato, and Ch. Baines, Phys. Rev. Lett. **93**, 217003 (2004).
[40] K. Kim and P. B. Weichman, Phys. Rev. B **43**, 13583 (1991).
[41] T. Schneider, in *High-Tc Superconductors and Related Transition Metal Oxides*, eds. A. Bussmann-Holder and H. Keller (Springer, Berlin, 2007), p. 269.
[42] Ch. Kittel, *Introduction to Solid State Physics* 7th ed., Wiley (1996).
[43] M. H. S. Amin, M. Franz, and I. Affleck, Phys. Rev. Lett. **84**, 5864 (2000).
[44] I. L. Landau and H. Keller, Physica C **466**, 131 (2007).
[45] Small and unphysical reduction ($\simeq 5\,\%$ in the field range of 50 to 640 mT) of λ with increasing field was obtained for the value of ξ determined from the corresponding B_{c2} (using the GL relation $B_{c2} = \Phi_0/2\pi\xi^2$). Such deviation rather points to a slight systematic deviation of vortex lattice field distribution from that of the ideal GL vortex lattice.
[46] P. Das, C. V. Tomy, S. S. Banerjee, H. Takeya, S. Ramakrishnan, and A. K. Grover, Phys. Rev. B **78**, 214504 (2008).
[47] R. Gumeniuk, K. O. Kvashnina, W. Schnelle, M. Nicklas, H. Borrmann, H. Rosner, Y. Skourski, A. A. Tsirlin, A. Leithe-Jasper, and Yu. Grin, J. Phys.: Condens. Matter **23**, 465601 (2011)
[48] R. T. Khan, E. Bauer, X.-Q. Chen, R. Podloucky, and P. Rogl, J. Phys. Soc. Jpn. **77** Suppl. A, 350 (2008).
[49] D. Saint-James and P. de Gennes, Phys. Lett. **7**, 306 (1963).
[50] R. Demchyna, Yu. Prots, W. Schnelle, U. Burkhardt, U. Schwarz, Z. Kristallogr. NCS **221**, 109 (2006).
[51] W. Schnelle, unpublished data.
[52] B. T. Matthias, T. H. Geballe, and V. B. Compton, Rev. Mod. Phys. **35**, 1 (1963).
[53] N. W. Ashcroft and N. D. Mermin, Solid State Physics, Harcourt College Publishers, Orlando FL (1976).
[54] For the charge carrier concentration we assume $n = 4$ electron holes per cell ($Z = 2$) for $BaPt_4Ge_{12}$ and a decrease of n to only 2 when one Pt atom is substituted by Au.
[55] A. A. Abrikosov, Sov. Phys. JETP **5**, 1174 (1957).
[56] E. H. Brandt, Phys. Rev. B **37**, 2349 (1988).

[57] A. D. Sidorenco, V. P. Smilga, and V. I. Fesenko, Hyperfine Interactions **63**, 49 (1990).
[58] Z. Hao, J. R. Clem, M. W. McElfresh, L. Civale, A. P. Malozemoff, and F. Holtzberg, Phys. Rev. B **43**, 2844 (1991)
[59] A. Yaouanc, P. Dalmas de Réotier and E. H. Brandt, Phys. Rev. B **55**, 11107 (1997).
[60] P. Dalmas De Réotier and A. Yaouanc, J. Phys.: Condens. Matter **9**, 9113 (1997).
[61] J. E. Sonier, J. H. Brewer, and R. F. Kiefl, Rev. Mod. Phys. **72**, 769 (2000).
[62] M. Laulajainen, F. D. Callaghan, C. V. Kaiser, and J. E. Sonier, Phys. Rev. B **74**, 054511 (2006).
[63] P. G. De Gennes, *Superconductivity of Metalls and Alloys*, Westview Press, Boulder CO (1999).